НАУЧНО-ТЕХНИЧЕСКИЙ ВЕСТНИК ИНФОРМАЦИОННЫХ ТЕХНОЛОГИЙ, МЕХАНИКИ И ОПТИКИ
ноябрь–декабрь 2023 Том 23 № 6 http://ntv.ifmo.ru/
SCIENTIFIC AND TECHNICAL JOURNAL OF INFORMATION TECHNOLOGIES, MECHANICS AND OPTICS
November–December 2023 Vol. 23 No 6 http://ntv.ifmo.ru/en/
ISSN 2226-1494 (print) ISSN 2500-0373 (online)

doi: 10.17586/2226-1494-2023-23-6-1114-1121

Structural analysis of ZrO_2 and TiO_2 nanoparticles

Gunel Imanova[1,2]✉

[1] Institute of Radiation Problems, Ministry of Science and Education Republic of Azerbaijan, Baku, AZ1143, Azerbaijan
[2] UNEC Research Center for Sustainable Development and Green Economy named after Nizami Ganjavi, Baku, AZ1001, Azerbaijan

gunel_imanova55@mail.ru✉, https://orcid.org/0000-0003-3275-300X

Abstract
The constituent parts of systems where radiation-catalytic processes occur usually differ in terms of mass and electron density, structural characteristics, electrophysical and chemical properties. Therefore, interaction between phases in any form has a sharp effect on the direction and parameters of the processes in individual components. In this work, X-ray diffraction patterns of nano-ZrO_2 and nano-TiO_2 samples were obtained before and after gamma irradiation. The crystal structures of these samples have been studied. The resulting X-ray diffraction pattern was mainly determined by the atomic plane (ε), the intensity of the obtained peaks, the corresponding syngony of the sample, the lattice size, density, lattice constants, and the distance between the phase groups. The X-ray diffraction data were processed using the Fullprof program. Full-profile processing of ZrO_2 X-ray diffraction data showed that the initial sample has a monoclinic structure (space group P21/*c*) with the following lattice parameters: a = 5.1506 Å, b = 5.2080 Å, c = 5.3293 Å. Full-profile processing of X-ray diffraction analysis of ZrO_2 after gamma irradiation showed a change in the structure from the monoclinic (space group P21/*c*) phase to the triclinic (space group P1). Full profile processing of TiO_2 X-ray diffraction data showed that the sample has a tetragonal structure (space group P42/mnm) with the following lattice parameters: $a = b$ = 4.5931 Å, c = 2.9592 Å and unit cell. As a result of calculations (B_R = 1.27; R_F = 1.98; χ^2 = 2.68), it was found that the structure of the initial TiO_2 sample is single-phase, tetragonal, and is described by the space group P42/mnm. Crystal structure of ZrO_2 (monoclinic structures, space group P21/*c*). Crystal structure of TiO_2 (tetragonal structure space group P42/mnm). The scientific component of the article is of interest because it touches upon the issues of structural transformations of zirconium oxide and titanium under the action of gamma radiation.

Keywords
nano-ZrO_2, nano-TiO_2, X-ray diffraction, crystal structure, gamma radiation

Acknowledgements
I express my gratitude to Farhad Khallokov, scientist of "Institute of Nuclear Physics of the Academy of Sciences of the Republic of Uzbekistan", and Ilkhom Bekpulatov, scientist of "Tashkent State Technical University", for helping me in the research conducting.

For citation: Imanova G. Structural analysis of ZrO_2 and TiO_2 nanoparticles. *Scientific and Technical Journal of Information Technologies, Mechanics and Optics*, 2023, vol. 23, no. 6, pp. 1114–1121. doi: 10.17586/2226-1494-2023-23-6-1114-1121

УДК 676.014.8

Структурный анализ наночастиц ZrO_2 и TiO_2

Гюнель Иманова[1,2]✉

[1] Институт Радиационных Проблем, Министерство науки и образования Азербайджанской Республики, Баку, AZ1143, Азербайджан
[2] Исследовательский центр UNEC по устойчивому развитию и зеленой экономике имени Низами Гянджеви, Баку, AZ1001, Азербайджан

gunel_imanova55@mail.ru✉, https://orcid.org/0000-0003-3275-300X

Аннотация
Введение. Составные части систем, в которых протекают радиационно-каталитические процессы, обычно различаются по массе и электронной плотности, структурным характеристикам, электрофизическим

и химическим свойствам. По этой причине взаимодействие фаз в любой форме оказывает большое влияние на направление и параметры процессов в отдельных компонентах. В работе получены рентгенограммы образцов нано-ZrO_2 и нано-TiO_2 до и после гамма-облучения. Исследованы их кристаллические структуры. **Метод.** Характер полученной рентгенограммы определялся атомной плоскостью (ε), интенсивностью полученных пиков, соответствующей сингонией образца, размером решетки, плотностью, постоянными решетки и расстоянием между фазовыми группами. Полученные данные рентгеноструктурного анализа обработаны с помощью программы Fullprof. **Основные результаты.** Полнопрофильная обработка данных рентгеноструктурного анализа оксида циркония (ZrO_2) показала, что исходный образец имеет моноклинную структуру (пространственная группа P21/*c*) со следующими параметрами решетки: *a* = 5,1506 Å, *b* = 5,2080 Å, *c* = 5,3293 Å. Полнопрофильная обработка рентгеноструктурного анализа ZrO_2 после гамма-облучения показала изменение структуры с моноклинной (пространственная группа P21/*c*) фазы на триклинную (пространственная группа P1). Полнопрофильная обработка данных рентгеноструктурного анализа оксида титана (TiO_2) показала, что образец имеет тетрагональную структуру (пространственная группа P42/mnm) со следующими параметрами решетки: *a* = *b* = 4,5931 Å, *c* = 2,9592 Å и элементарной ячейкой. В результате расчетов (B_R = 1,27; R_F = 1,98; χ_2 = 2,68) установлено, что структура исходного образца TiO_2 является однофазной, тетрагональной и описывается пространственной группой P42/mnm. **Обсуждение.** Таким образом, в работе показаны структурные превращения оксидов циркония и титана под действием гамма-излучения.

Ключевые слова
нано-ZrO_2, нано-TiO_2, рентгеновская дифракция, кристаллическая структура, гамма-излучение

Благодарности
Выражаю благодарность Фархад Халлокову научному сотруднику «Института ядерной физики Академии наук Республики Узбекистан» и Ильхом Бекпулатову научному сотруднику «Ташкентского государственного технического университета» за помощь в проведении исследований.

Ссылка для цитирования: Иманова Г. Структурный анализ наночастиц ZrO_2 и TiO_2 // Научно-технический вестник информационных технологий, механики и оптики. 2023. Т. 23, № 6. С. 1114–1121 (на англ. яз.). doi: 10.17586/2226-1494-2023-23-6-1114-1121

Introduction

Nanometer-scale materials have recently attracted considerable scientific attention because of their beneficial high surface to volume ratio and therefore unique chemical, electronic, and physical properties. In particular titanium dioxide (TiO_2) nanoparticles are in the focus of research and thus many reports on electrical, optical, and structural properties of TiO_2 nanoparticles can be found [1–7]. Most of the research reports on the structural properties of nanoparticles dealt with the determination of structure type, physical and different microstructural parameters. X-ray diffraction line broadening studies give more useful information about the physical parameters such as crystallite size, dislocation density and strain [8–14]. TiO_2 is one of the most important materials having various important applications, such as water and air purification, self-cleaning materials and photovoltaic cells. TiO_2 is an *n*-type semiconductor having a wide band gap (3.2 eV for anatase and 3.0 eV for rutile). Deposition of thin films of TiO_2 doped with Mn on F-doped SnO_2-coated glass by spin coating has been described. Deposition of thin films of TiO_2 on various substrates by a simple sol-gel dip coating technique has been proposed. It has various photo-catalytic applications where it can be used in two forms, i.e., as highly dispersed fine particles on porous support materials and as suspended fluids in liquid medium. Titanium (IV) oxide is a white colored compound which can be used as a coloring pigment in paints and a main ingredient of cosmetics and toothpaste. It can be prepared via reaction of titanium (IV) chloride with oxygen gas. It can also find applications in photovoltaics, photocatalysis and gas sensors. TiO_2 is a semiconductor oxide with attractive photoactivity properties under UV irradiation [15–20].

The two most studied forms of titania, rutile and anatase are photoactive [21–26]. The gap of anatase is equal to 3.23 eV whereas the gap of rutile is equal to 3.02 eV [27]. Anatase is known to be the most photoactive TiO_2 polymorphic material, but, however, it is widely used as pigments and fillers in polymer materials and coatings. Nevertheless, mixtures of both phases showed particular efficacy, for instance, the standard nano-powder P25, from Degussa, is a mixture of 80 % anatase and 20 % rutile [28–30]. This formulation limits the recombination of charges due to the lower gap of rutile, however, their photocatalytic activity depends on the compounds to be degraded; the affinity of anatase in term of adsorption of organic compounds and polymers with the particle surface is one of the most important causes of the degradation activity [31, 32]. Many reports have clarified that the photocatalytic activity of TiO_2 strongly depends on its physical properties, surface area, crystallinity, and surface acidity, to name a few [33, 34]. The correlation between the photocatalytic activity and the physical properties of TiO_2 powders, such as crystal structure, surface area, crystallite size, and surface hydroxyl groups for example, has been accepted [35–37]. It is believed that the crystal structure is one of the most basic properties used to predict the photocatalytic activity; however, the main property that plays an important role is also well-known to be the surface area and the surface chemistry [38]. It has been well accepted that surface area contact is an essential factor for the effectiveness of the catalyst. Therefore, it is considered essential to have a nano-powder, in this case, which will have the smallest crystallite size in order to enhance the surface area of contact and therefore the photocatalytic activity [39–42].

Generally, the latter approach deserves a more attention in the future because it might bring new information

about the details of grain boundary evolution during the sintering ceramic materials. The energetics of formation and migration of the oxygen vacancy and interstitial in cubic zirconium dioxide (ZrO_2) are investigated by density functional theory calculations. In an O-rich environment, the negatively charged oxygen interstitial is the most dominant defect, whereas the positively charged oxygen vacancy is the most dominant defect under O-poor conditions. Oxygen interstitial migration occurs by the interstitially and the direct interstitial mechanisms, with calculated migration energy barriers of 2.94 eV and 2.15 eV, respectively. Some novel activity and crystal structure properties are observed and reported showing the anatase polymorph to exhibit high thermodynamic stability. For some nano-rutile particles photoactivity and crystal size has an unusual limitation below 25 nm where photoactivity decreases. This effect is confirmed from both methyl orange dye fading kinetics and solid-state analysis and weathering on doped isocyanate-acrylic paint films.

In the study work, XRD pattern of nano-ZrO_2 and nano-TiO_2 samples were taken before and after gamma irradiation. Crystal structures of those samples were studied.

Materials and method

As a research object, the nanoscale TiO_2 with a purity of 99.999 %, bulk density of 0.069 g/cm^3, specific surface area 70–90 m^2/g, and particle size to 20–30 nm (Sigma–Aldrich, Germany), the purity rate of nanoscale ZrO_2 was 99.9 % (Sky Spring Nanomaterials, USA), d = 20–30 nm, density ρ = 0.4–0.6 g/cm^3 and special surface area S = 330 m^2/g was used in this work. X-ray diffraction studies were carried out on a Malvern Panalytical Empyrean diffractometer. XRD data were recorded using a Malvern Panalytical Empyrean analytical diffractometer with CuKα radiation (λ = 1.54 Å). In this experiment, the accelerating voltage of the radiation generator was set to 45 kV and the emission current to 40 mA. X-ray diffraction patterns were recorded in Bragg-Brentano beam geometry at 2θ = 20°–70° continuously at a scan rate of 0.43 degrees/min. The resulting X-ray diffraction pattern was mainly determined by the lattice strain (ε), the intensity of the obtained peaks, the corresponding syngony of the sample, the lattice size, density, lattice constants, and the distance between the phase groups. The lattice parameters are calculated based on the square formulas of crystallography [15, 18, 29]. Irradiation of ZrO_2 and TiO_2 samples was carried out in a gamma device with ^{60}Co sources (E_{av} = 1.25 MeV) at a dose rate of 75 R/s, up to an exposure dose of 10^6 R.

Results and discussion

Nano-ZrO_2. The X-ray diffraction data were processed using the Fullprof program. The results of measurement and processing of X-ray diffraction data are shown in Fig. 1 and Table 1.

Full-profile processing of ZrO_2 X-ray diffraction data showed that the initial sample has a monoclinic structure (space group P21/c) with the following lattice parameters: a = 5.1506 Å, b = 5.2080 Å, c = 5.3293 Å and unit cell (Table 1). Here, x, y, and z represent the size of the atoms. As a result of calculations (B_R = 1.78; R_F = 1.59; χ_2 = 2.71), it was found that the structure of the original ZrO_2 sample is single-phase, monoclinic, and is described by the space group P21/c (Fig. 1, Intensity is in arbitrary units, a.u.).

The unit cell of the ZrO_2 monoclinic structure is shown in Fig. 2 and Table 2.

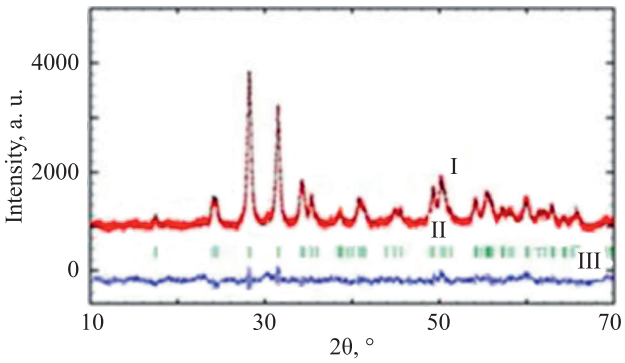

Fig. 1. X-ray diffraction pattern of the original ZrO_2 sample: I — experimental and calculated data; II — Bragg reflections; III — difference curve between experimental and calculated data

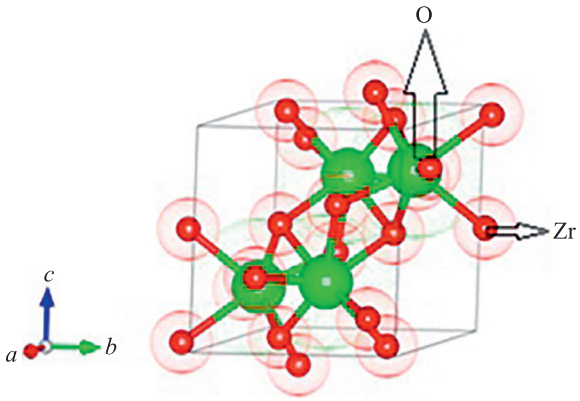

Fig. 2. Crystal structure of ZrO_2 (monoclinic structures, space group P21/c)

Table 1. X-ray diffraction data

Molecule	Coordinates of atoms			Thermal factor B
	x/a	y/b	z/c	
Zr	0.2763	0.0421	0.2096	0.4028
O_1	0.0692	0.1662	0.8438	0.9572
O_2	0.4493	0.7425	0.9786	0.5355

Table 2. Properties of gamma-irradiated ZrO_2

Sample	2θ, °	β_s,°	*D*, nm	δ ×10^{15}, lines/m^2	ε, %
Initial ZrO_2	28.128	0.506	15.23	4.31	0.88
Gamma-irradiated ZrO_2	28.134	0.513	15.02	4.43	0.89

Based on the obtained powder X-ray diffraction data, the size of crystallites was determined using the Scherrer formula.

$$D = \frac{k\lambda}{\beta_S \cos\theta},$$

where *D* is the average crystallite size, *k* is the geometric coefficient (0.9), λ is the X-ray wavelength (1.5406 Å), β_s is the diffraction reflection width at half maximum (FWHM), and θ is the diffraction angle.

The dislocation density was determined from the equation:

$$\delta = 1/D^2.$$

The microstress value in ZrO_2 was calculated using the Stokes-Wilson equation:

$$\varepsilon = \frac{\beta}{4\tan\theta}.$$

Full-profile processing of X-ray diffraction analysis of ZrO_2 after gamma irradiation showed a change in the structure from the monoclinic (space group P21/*c*) phase to the triclinic (space group P1). As a result (Fig. 3 and Fig. 4) of calculations of the irradiated ZrO_2 sample, the combination (B_R = 1.13; R_F = 2.52; χ^2 = 1.88) was found.

On the other hand, the electronic properties investigations show that the displacement of oxygen atoms for tetragonal structure leads to half of the zirconium–oxygen bonds becoming stronger and the other half weaker

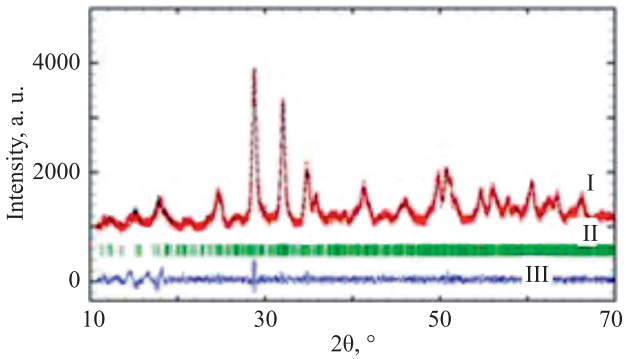

Fig. 3. X-ray pattern of an irradiated ZrO_2 sample: I — experimental and calculated data; II — Bragg reflections; III — difference curve between experimental and calculated data

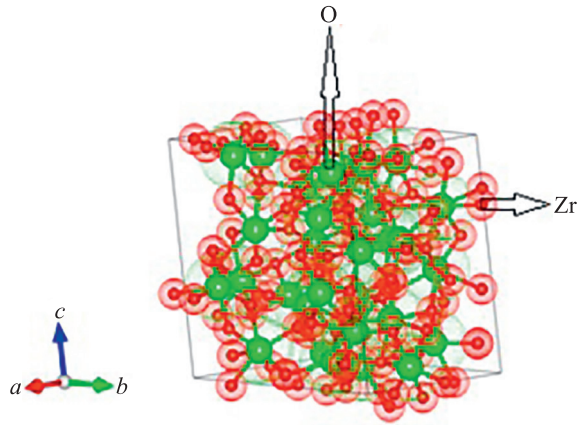

Fig. 4. Crystal structure of ZrO_2 (triclinic structures, space group P1)

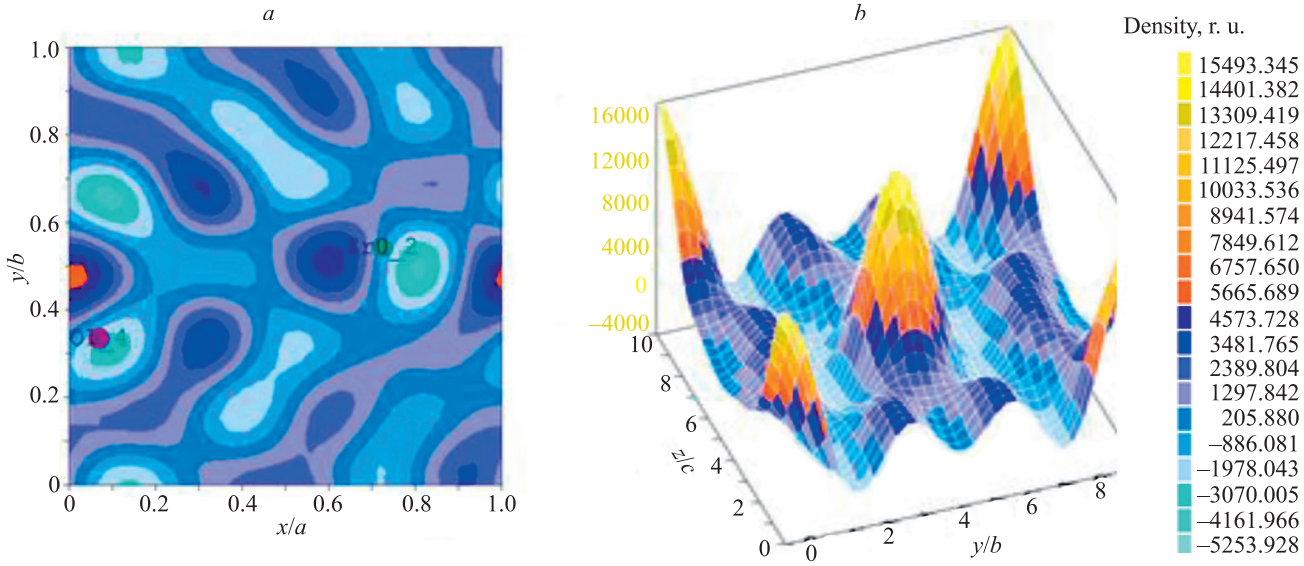

Fig. 5. 2D (*a*) and 3D (*b*) view of electron density maps of ZrO_2

when they are compared with the bonds in cubic zirconia. According to the band structure calculations of different zirconia phases, the cotunnite structure is supposed to be better than the other ones as gate dielectric material (Fig. 5, Density is in relative units, r.u.).

Nano-TiO_2. The X-ray diffraction data were processed using the Fullprof program. The results of measurement and processing of X-ray diffraction data are shown in Fig. 6 and in Table 3.

Full-profile processing of TiO_2 X-ray diffraction data showed that the sample has a tetragonal structure (space group P42/mnm) with the following lattice parameters: $a = b = 4.5931$ Å, $c = 2.9592$ Å and unit cell (Table 3). As a result of calculations ($B_R = 1.27$; $R_F = 1.98$; $\chi^2 = 2.68$), it was found that the structure of the initial TiO_2 sample is single-phase, tetragonal, and is described by the space group P42/mnm (Table 4). The elementary cell of the tetragonal TiO_2 structure is shown in Fig. 7.

Full-profile processing of X-ray diffraction data of TiO_2 after gamma irradiation (Fig. 8) shows that the lattice parameters increase: $a = b = 4.5946$ Å, $c = 2.9609$ Å and tetragonal showed that it has a structure (space group P42/mnm) and unit cell (Table 5) as a result of calculations of the irradiated TiO_2 sample ($B_R = 1.09$; $R_F = 2.67$; $\chi_2 = 1.77$).

Ionizing radiation is often more energetic than non-ionizing radiation and, as a result, is more likely to induce electronic transitions of atoms and molecules. In electronic excitation, an electron absorbing the radiation transits into a higher electronic state becoming less bounded to the nucleus and therefore more reactive. If the radiation has sufficient energy, the electron can escape the coulomb attraction of the nucleus, and the molecule is ionized. In contrast, molecules undergoing rotational or vibrational transitions experience minimal changes in the stability of the electron-nucleus attraction, resulting in negligible chemical effects. Therefore, the scientific component of the article is of interest because it touches upon the issues of structural transformations of zirconium oxide and titanium under the action of gamma radiation.

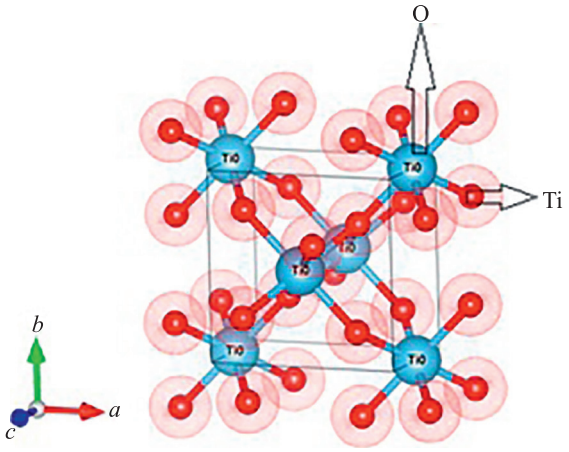

Fig. 7. Crystal structure of TiO_2 (tetragonal structure space group P42/mnm)

Table 4. Properties of gamma-irradiated TiO_2

Impact external physical parameters	Initial	Gamma radiation $\times 10^6$, Gy
D, nm	0.68	0.33
$\sigma \times 10^{14}$, m^{-2}	0.02	0.09

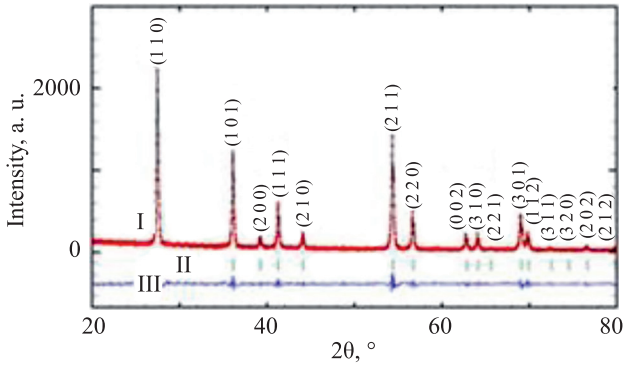

Fig. 6. X-ray diffraction pattern of the original TiO_2 sample. I — experimental and calculated data; II — Bragg reflections; III — difference curve between experimental and calculated data

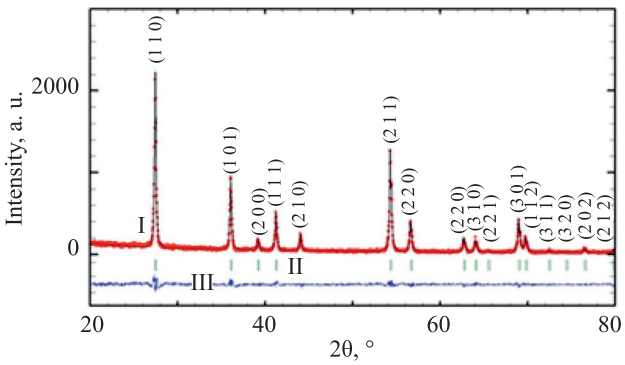

Fig. 8. X-ray pattern of an irradiated TiO_2 sample: I — experimental and calculated data; II — Bragg reflections; III — difference curve between experimental and calculated data

Table 3. X-ray diffraction data

Molecule	Coordinates of atoms			Thermal factor B
	x/a	y/b	z/c	
Ti	0.00000	0.00000	0.50000	0.15676
O_2	0.19568	0.80432	0.00000	0.16562

Table 5. X-ray diffraction data of the irradiated TiO_2 sample

Molecule	Coordinates of atoms			Thermal factor B
	x/a	y/b	z/c	
Ti	0.00000	0.00000	0.50000	0.36946
O_2	0.19568	0.80432	0.00000	0.24743

Conclusion

The study full-profile processing of ZrO_2 X-ray diffraction data showed that the initial sample has a monoclinic structure (space group P21/*c*) with the following lattice parameters: $a = 5.1506$ Å, $b = 5.2080$ Å, $c = 5.3293$ Å. X-ray diffraction analysis of ZrO_2 after gamma irradiation showed a change in the structure from the monoclinic (space group P21/*c*) phase to the triclinic (space group P1). As a result of calculations of the irradiated ZrO_2 sample, the combination ($B_R = 1.13$; $R_F = 2.52$; $\chi^2 = 1.88$) was found. Full-profile processing of TiO_2 X-ray diffraction data showed that the sample has a tetragonal structure (space group P42/mnm) with the following lattice parameters: $a = b = 4.5931$ Å, $c = 2.9592$ Å and unit cell. As a result of calculations with combination ($B_R = 1.27$; $R_F = 1.98$; $\chi^2 = 2.68$), it was found that the structure of the initial TiO_2 sample is single-phase, tetragonal, and is described by the space group P42/mnm. Full-profile processing of X-ray diffraction data of TiO_2 after gamma irradiation shows that the lattice parameters increase: $a = b = 4.5946$ Å, $c = 2.9609$ Å and tetragonal showed that it has a structure (space group P42/mnm), unit cell (Table 5) as a result of calculations of the irradiated TiO_2 sample ($B_R = 1.09$; $R_F = 2.67$; $\chi^2 = 1.77$). Crystal structure of ZrO_2 is monoclinic structure (space group P21/*c*). Crystal structure of TiO_2 is tetragonal structure (space group P42/mnm).

References

1. Mustafayev I.I., Mahmudov H.M. Radiation-thermal desulphurization of organic fuels. *Journal of Radiation Researches*, 2015, vol. 2, no. 2, pp. 65–70.
2. Mahmudov H.M., Suleymanov T.Y., Aliyev S.M., Huseynova S.A., Azizova K.V., Mammadova B.M. Kinetics and mechanism of formation of gaseous products obtained by radiation-catalytic conversion of n-hexane on the surface of nano-ZrO_2. *Journal of Radiation Research*, 2018, vol. 5, no. 2, pp. 119–125.
3. Imanova G.T. Kinetics of radiation-heterogeneous and catalytic processes of water in the presence of zirconia nanoparticles. *Advanced Physical Research*, 2020, vol. 2, no. 2, pp. 94–101.
4. Imanova G.T. Gamma rays mediated hydrogen generation by water decomposition on nano-ZrO_2 surface. *Modern Approaches on Material Science*, 2021, vol. 4, no. 3, pp. 508–514. https://doi.org/10.32474/MAMS.2021.04.000186
5. Jabbarova L.Y., Mustafayev I.I., Akbarov R.Y., Mirzayeva A.S. Study of post-radiation processes in model hexane/hexene binary systems. *Journal of Radiation Research*, 2022, vol. 9, no. 1, pp. 58–63.
6. Musayeva Sh.Z. Impact of n-ZrO_2 on the radiolysis of hexane. *Journal of Radiation Researches*, 2021, vol. 8, no. 1, pp. 42–47.
7. Garibov A.A. Size effects in radiation-catalytic processes of water decomposition and perspectives of use of nanocatalysts in this field. *Journal of Radiation Researches*, 2014, vol. 1, no. 1, pp. 5–13.
8. Agayev T.N., Musayeva Sh.Z., Mahmudov H.M. Kinetics of accumulation of hydrocarbons and oxidation products during radiolysis of a mixture of water-hexan. *Journal of Radiation Researches*, 2018, vol. 5, no. 2, pp. 198–203.
9. Gulieva U.A., Gurbanov M.A., Mahmudov H.M. Study of radiation degradation of phenol in aqueous solution by uv spectroscopy. *Journal of Radiation Researches*, 2014, vol. 1, no. 1, pp. 76–79.
10. Garibov A.A., Agayev T.N., Imanova G.T. Nanostructured materials based on nano-ZrO_2 in the nuclear-power engineering. *Journal of Radiation Researches*, 2014, vol. 1, no. 1, pp. 50–56.
11. Garibov A.A., Agayev T.N., Mansimov Z.A., Eyyubov K.T. Influence of temperature and density of water vapor on the yield of molecular hydrogen in the presence of radium-silicate. *Journal of Radiation Researches*, 2014, vol. 1, no. 1, pp. 57–60.
12. Jafarov Y.D., Bashirova S.M., Aliyev S.M. The impact of mass and size effects on the water radiolysis process in Si + H_2O system. Journal of Radiation Researches, 2015, vol. 2, no. 2, pp. 21–26.
13. Agayev T.N., Huseynov V.I., Eyubov K.T. Research of high-temperature oxidation of zirconium by the thermo gravimetric method. *Journal of Radiation Researches*, 2017, vol. 4, no. 1, pp. 37–42.
14. Mahmudov H., Suleymanov T., Sabzaliyeva Z., Imanova G., Akhundzada H.V., Azizova K., Hasanova S., Hasanov S. Kinetic interaction of hexan conversion and oxidation on the surface of an Al_2O_3 nanocatalyzer at room temperature under the effect of gamma radiation. *Journal of Chemistry*, 2021, pp. 9493765. https://doi.org/10.1155/2021/9493765
15. Imanova G.T., Agayev T.N., Jabarov S.H. Investigation of structural and optical properties of zirconia dioxide nanoparticles by radiation and thermal methods. *Modern Physics Letters B*, 2021, vol. 35, no. 2, pp. 2150050. https://doi.org/10.1142/s0217984921500500

Литература

1. Mustafayev I.I., Mahmudov H.M. Radiation-thermal desulphurization of organic fuels // Journal of Radiation Researches. 2015. V. 2. N 2. P. 65–70.
2. Mahmudov H.M., Suleymanov T.Y., Aliyev S.M., Huseynova S.A., Azizova K.V., Mammadova B.M. Kinetics and mechanism of formation of gaseous products obtained by radiation-catalytic conversion of n-hexane on the surface of nano-ZrO_2 // Journal of Radiation Research. 2018. V. 5. N 2. P. 119–125.
3. Imanova G.T. Kinetics of radiation-heterogeneous and catalytic processes of water in the presence of zirconia nanoparticles // Advanced Physical Research. 2020. V. 2. N 2. P. 94–101.
4. Imanova G.T. Gamma rays mediated hydrogen generation by water decomposition on nano-ZrO_2 surface // Modern Approaches on Material Science. 2021. V. 4. N 3. P. 508–514. https://doi.org/10.32474/MAMS.2021.04.000186
5. Jabbarova L.Y., Mustafayev I.I., Akbarov R.Y., Mirzayeva A.S. Study of post-radiation processes in model hexane/hexene binary systems // Journal of Radiation Research. 2022. V. 9. N 1. P. 58–63.
6. Musayeva Sh.Z. Impact of n-ZrO_2 on the radiolysis of hexane // Journal of Radiation Researches. 2021. V. 8. N 1. P. 42–47.
7. Garibov A.A. Size effects in radiation-catalytic processes of water decomposition and perspectives of use of nanocatalysts in this field // Journal of Radiation Researches. 2014. V. 1. N 1. P. 5–13.
8. Agayev T.N., Musayeva Sh.Z., Mahmudov H.M. Kinetics of accumulation of hydrocarbons and oxidation products during radiolysis of a mixture of water-hexan // Journal of Radiation Researches. 2018. V. 5. N 2. P. 198–203.
9. Gulieva U.A., Gurbanov M.A., Mahmudov H.M. Study of radiation degradation of phenol in aqueous solution by uv spectroscopy // Journal of Radiation Researches. 2014. V. 1. N 1. P. 76–79.
10. Garibov A.A., Agayev T.N., Imanova G.T. Nanostructured materials based on nano-ZrO_2 in the nuclear-power engineering // Journal of Radiation Researches. 2014. V. 1. N 1. P. 50–56.
11. Garibov A.A., Agayev T.N., Mansimov Z.A., Eyyubov K.T. Influence of temperature and density of water vapor on the yield of molecular hydrogen in the presence of radium-silicate // Journal of Radiation Researches. 2014. V. 1. N 1. P. 57–60.
12. Jafarov Y.D., Bashirova S.M., Aliyev S.M. The impact of mass and size effects on the water radiolysis process in Si + H_2O system // Journal of Radiation Researches. 2015. V. 2. N 2. P. 21–26.
13. Agayev T.N., Huseynov V.I., Eyubov K.T. Research of high-temperature oxidation of zirconium by the thermo gravimetric method // Journal of Radiation Researches. 2017. V. 4. N 1. P. 37–42.
14. Mahmudov H., Suleymanov T., Sabzaliyeva Z., Imanova G., Akhundzada H.V., Azizova K., Hasanova S., Hasanov S. Kinetic interaction of hexan conversion and oxidation on the surface of an Al_2O_3 nanocatalyzer at room temperature under the effect of gamma radiation // Journal of Chemistry. 2021. P. 9493765. https://doi.org/10.1155/2021/9493765
15. Imanova G.T., Agayev T.N., Jabarov S.H. Investigation of structural and optical properties of zirconia dioxide nanoparticles by radiation and thermal methods // Modern Physics Letters B. 2021. V. 35. N 2. P. 2150050. https://doi.org/10.1142/s0217984921500500

16. Ali I., Imanova G.T., Garibov A.A., Agayev T.N., Jabarov S.H., Almalki A.SA., Alsubaie A. Gamma rays mediated water splitting on nano-ZrO_2 surface: Kinetics of molecular hydrogen formation. *Radiation Physics and Chemistry*, 2021, vol. 183, pp. 109431. https://doi.org/10.1016/j.radphyschem.2021.109431
17. Agayev T.N., Musayeva Sh.Z., Imanova G.T. Kinetics of formation of molecular hydrogen during the radiolysis of hexane and a mixture of C_6H_{14}–H_2O on a surface of ZrO_2 Nanoparticles. *Russian Journal of Physical Chemistry A*, 2021, vol. 95, no. 2, pp. 270–272. https://doi.org/10.1134/s0036024421020023
18. Imanova G.T., Agaev T.N., Garibov A.A., Melikova S.Z., Jabarov S.H., Akhundzada H.V. Radiation-thermocatalytic and thermocatalytic properties of n-ZrO_2-n-SiO_2 systems in the process of obtaining hydrogen from water at different temperatures. *Journal of Molecular Structure*, 2021, vol. 1241, pp. 130651. https://doi.org/10.1016/j.molstruc.2021.130651
19. Ali I., Imanova G.T., Mbianda X.Y., Alharbi O.M.L. Role of the radiations in water splitting for hydrogen generation. *Sustainable Energy Technologies and Assessments*, 2022, vol. 51, pp. 101926. https://doi.org/10.1016/j.seta.2021.101926
20. Ali I., Imanova G.T., Albishri H.M., Alshitari W.H., Locatelli M., Siddiqui M.N., Hameed A.M. An ionic-liquid-imprinted nanocomposite adsorbent: Simulation, kinetics and thermodynamic studies of triclosan endocrine disturbing water contaminant removal. *Molecules*, 2022, vol. 27, no. 17, pp. 5358. https://doi.org/10.3390/molecules27175358
21. Tursunmetova Z.A., Imanova G., Bekpulatov I. Method for low-temperature vacuum-thermal cleaning of surface single crystals Si and GaAs. *Journal of Polytechnic*, 2022, vol. 25, no. 2, pp. 921–927. https://doi.org/10.2339/politeknik.1119884
22. Ali I., Imanova G., Agayev T., Aliyev A., Alharbi O.M.L., Alsubaie A., Almalki A.S.A. A comparison of hydrogen production by water splitting on the surface of α-, δ- and γ-Al_2O_3. *ChemistrySelect*, 2022, vol. 7, no. 34, pp. e202202618. https://doi.org/10.1002/slct.202202618
23. Ali I., Imanova G., Agayev T., Aliyev A., Jabarov S., Albishri H.M., Alshitari W.H., Hameed A.M., Alharbi A. Seawater splitting for hydrogen generation using zirconium and its niobium alloy under gamma radiation. *Molecules*, 2022, vol. 27, no. 19, pp. 6325. https://doi.org/10.3390/molecules27196325
24. Imran A., Imanova G. Sorbtion: A universal technology for water purification. *Advanced Physical Research*, 2022, vol. 4, no. 1, pp. 5–9.
25. Agayev T., Imanova G., Aliyev A. Influence of gamma radiation on current density and volt–ampere characteristics of metallic zirconium. *International Journal of Modern Physics B*, 2022, vol. 36, no. 19, pp. 2250115. https://doi.org/10.1142/s0217979222501156
26. Ali I., Mahmudov H., Imanova G., Suleymanov T., Hameed A.M., Alharbi A. Hydrogen production on nano Al_2O_3 surface by water splitting using gamma radiation. *Journal of Chemical Technology & Biotechnology*, 2023, vol. 98. no. 2, pp. 1186–1191. https://doi.org/10.1002/jctb.7322
27. Barkaoui S., Haddaoui M., Dhaouadi H., Raouafi N., Touati F. Hydrothermal synthesis of urchin-like Co_3O_4 nanostructures and their electrochemical sensing performance of H_2O_2. *Journal of Solid State Chemistry*, 2015, vol. 228, pp. 226–231. https://doi.org/10.1016/j.jssc.2015.04.043
28. Barkaoui S., Dhaouadi H., Kouass S., Touati F. Structural and optical proprieties of doped cobalt oxide: $CuxCo_3$-xO_4 (x = 0.0; 0.1; 0.2; 0.4; and 0.6). *Optik*, 2015, vol. 126, no. 9-10, pp. 1047–1051. https://doi.org/10.1016/j.ijleo.2015.02.056
29. Imanova G., Asgerov E., Jabarov S., Mansimov Z., Kaya M., Doroshkevich A. Hydrogen generation during thermal processes of water decomposition on the surface of nano-ZrO_2 + 3mol.%Y_2O_3. *Trends in Sciences*, 2023, vol. 20, no. 4, pp. 4684. https://doi.org/10.48048/tis.2023.4684
30. Ali I., Agayev T., Imanova G., Mahmudov H., Musayeva Sh., Alharbi O.M.L., Siddiqui M.N. Effective hydrogen generation using water-n-hexane-ZrO_2 system: Effect of temperature and radiation irradiation time. *Materials Letters*, 2023, vol. 340, pp. 134188. https://doi.org/10.1016/j.matlet.2023.134188
31. Bekpulatov I.R., Imanova G.T., Kamilov T.S., Igamov B.D., Turapov I.Kh. Formation of n-type CoSi monosilicide film which can be used in instrumentation. *International Journal of Modern Physics B*, 2023, vol. 37, no. 17, pp. 22350164. https://doi.org/10.1142/s0217979223501643

16. Ali I., Imanova G.T., Garibov A.A., Agayev T.N., Jabarov S.H., Almalki A.SA., Alsubaie A. Gamma rays mediated water splitting on nano-ZrO_2 surface: Kinetics of molecular hydrogen formation // Radiation Physics and Chemistry. 2021. V. 183. P. 109431. https://doi.org/10.1016/j.radphyschem.2021.109431
17. Agayev T.N., Musayeva Sh.Z., Imanova G.T. Kinetics of formation of molecular hydrogen during the radiolysis of hexane and a mixture of C_6H_{14}–H_2O on a surface of ZrO_2 Nanoparticles // Russian Journal of Physical Chemistry A. 2021 V. 95. N 2. P. 270–272. https://doi.org/10.1134/s0036024421020023
18. Imanova G.T., Agaev T.N., Garibov A.A., Melikova S.Z., Jabarov S.H., Akhundzada H.V. Radiation-thermocatalytic and thermocatalytic properties of n-ZrO_2-n-SiO_2 systems in the process of obtaining hydrogen from water at different temperatures // Journal of Molecular Structure. 2021. V. 1241. P. 130651. https://doi.org/10.1016/j.molstruc.2021.130651
19. Ali I., Imanova G.T., Mbianda X.Y., Alharbi O.M.L. Role of the radiations in water splitting for hydrogen generation // Sustainable Energy Technologies and Assessments. 2022. V. 51. P. 101926. https://doi.org/10.1016/j.seta.2021.101926
20. Ali I., Imanova G.T., Albishri H.M., Alshitari W.H., Locatelli M., Siddiqui M.N., Hameed A.M. An ionic-liquid-imprinted nanocomposite adsorbent: Simulation, kinetics and thermodynamic studies of triclosan endocrine disturbing water contaminant removal // Molecules. 2022. V. 27. N 17. P. 5358. https://doi.org/10.3390/molecules27175358
21. Tursunmetova Z.A., Imanova G., Bekpulatov I. Method for low-temperature vacuum-thermal cleaning of surface single crystals Si and GaAs // Journal of Polytechnic. 2022. V. 25. N 2. P. 921–927. https://doi.org/10.2339/politeknik.1119884
22. Ali I., Imanova G., Agayev T., Aliyev A., Alharbi O.M.L., Alsubaie A., Almalki A.S.A. A comparison of hydrogen production by water splitting on the surface of α-, δ- and γ-Al_2O_3 // ChemistrySelect. 2022. V. 7. N 34. P. e202202618. https://doi.org/10.1002/slct.202202618
23. Ali I., Imanova G., Agayev T., Aliyev A., Jabarov S., Albishri H.M., Alshitari W.H., Hameed A.M., Alharbi A. Seawater splitting for hydrogen generation using zirconium and its niobium alloy under gamma radiation // Molecules. 2022. V. 27. N 19. P. 6325. https://doi.org/10.3390/molecules27196325
24. Imran A., Imanova G. Sorbtion: A universal technology for water purfication // Advanced Physical Research. 2022. V. 4. N 1. P. 5–9.
25. Agayev T., Imanova G., Aliyev A. Influence of gamma radiation on current density and volt–ampere characteristics of metallic zirconium // International Journal of Modern Physics B. 2022. V. 36. N 19. P. 2250115. https://doi.org/10.1142/s0217979222501156
26. Ali I., Mahmudov H., Imanova G., Suleymanov T., Hameed A.M., Alharbi A. Hydrogen production on nano Al_2O_3 surface by water splitting using gamma radiation // Journal of Chemical Technology & Biotechnology. 2023. V. 98. N 2. P. 1186–1191. https://doi.org/10.1002/jctb.7322
27. Barkaoui S., Haddaoui M., Dhaouadi H., Raouafi N., Touati F. Hydrothermal synthesis of urchin-like Co_3O_4 nanostructures and their electrochemical sensing performance of H_2O_2 // Journal of Solid State Chemistry. 2015. V. 228. P. 226–231. https://doi.org/10.1016/j.jssc.2015.04.043
28. Barkaoui S., Dhaouadi H., Kouass S., Touati F. Structural and optical proprieties of doped cobalt oxide: $CuxCo_3$-xO_4 (x = 0.0; 0.1; 0.2; 0.4; and 0.6) // Optik. 2015. V. 126. N 9-10. P. 1047–1051. https://doi.org/10.1016/j.ijleo.2015.02.056
29. Imanova G., Asgerov E., Jabarov S., Mansimov Z., Kaya M., Doroshkevich A. Hydrogen generation during thermal processes of water decomposition on the surface of nano-ZrO_2 + 3mol.%Y_2O_3 // Trends in Sciences. 2023. V. 20. N 4. P. 4684. https://doi.org/10.48048/tis.2023.4684
30. Ali I., Agayev T., Imanova G., Mahmudov H., Musayeva Sh., Alharbi O.M.L., Siddiqui M.N. Effective hydrogen generation using water-n-hexane-ZrO_2 system: Effect of temperature and radiation irradiation time // Materials Letters. 2023. V. 340. P. 134188. https://doi.org/10.1016/j.matlet.2023.134188
31. Bekpulatov I.R., Imanova G.T., Kamilov T.S., Igamov B.D., Turapov I.Kh. Formation of n-type CoSi monosilicide film which can be used in instrumentation // International Journal of Modern Physics B. 2023. V. 37. N 17. P. 22350164. https://doi.org/10.1142/s0217979223501643

32. Umirzakov B.E., Imanova G.T., Bekpulatov I.R., Turapov I.Kh. Obtaining of thin films of manganese silicides on a Si surface by the method of solid-phase deposition and investigation of their electronic structure. *Modern Physics Letters B*, 2023, vol. 37, no. 24, pp. 2350078. https://doi.org/10.1142/S0217984923500781
33. Mansimov Z., Imanova G., Garibov A., Agayev T. investigation of radiation-heterogeneous and catalytic processes in the surface of $(RaO)x(SiO_2)y + H_2O$ system. *Journal of the Turkish Chemical Society Section A: Chemistry*, 2023, vol. 10, no. 2, pp. 487–492. https://doi.org/10.18596/jotcsa.1118855
34. Barkaoui S., Chakhari S., Kouass S., Dhaouadi H., Imanova G., Touati F. Influence of Ag-doping-cobalt oxide on the structure, optical properties, morphology and preferential oxidation activity of CO. *Advanced Physical Research*, 2022, vol. 4, no. 1, pp. 22–32.
35. Canpolat G., Ziyadanoğullari R. Recovery of copper from complex copper oxide ore by flotation and leaching methods. *Advanced Physical Research*, 2023, vol. 5, no. 2, pp. 103–116.
36. Teng F., Chen M., Li G., Teng Y., Xu T., Hang Y., Yao W., Santhanagopalan S., Meng D.D., Zhu Y. High combustion activity of CH_4 and catalluminescence properties of CO oxidation over porous Co_3O_4 nanorods. *Applied Catalysis B: Environmental*, 2011, vol. 110, pp. 133–140. https://doi.org/10.1016/j.apcatb.2011.08.035
37. Che H., Liu A., Fu Q., Jiang R. Facile synthesis of porous cobalt oxide microdiscs and their catalytic property in CO oxidation. *Materials Letters*, 2013, vol. 93, pp. 240–243. https://doi.org/10.1016/j.matlet.2012.11.108
38. Barkaoui S., Imanova G. Hydrothermal synthesis of Co_3O_4 urchin-like and their catalytic properties in CO oxidation. *Juniper Online Journal Material Science*, 2022, vol. 7, no. 1, pp. 555704. https://doi.org/10.19080/jojms.2022.07.555704
39. Popov E.P., Aliyev O.A., Demir E., Neov D., Doroshkevich A.S., Mirzayev M.N., Horodek P., Thabethe T.T., Imanova G.T., Akhundzada H.V., Sidorin A.A., Mamedov F. Kinetics of thermo heterogeneous process under non-isothermal terms on the titanium carbide: a study on the different irradiation conditions. *Advanced Physical Research*, 2022, vol. 4, no. 2, pp. 81–86.
40. Aliyev Y.I., Dashdemirov A.O., Novruzov R.F. Structural phase transitions in the compound $Ag_{1.55}Cu_{0.45}S$ at high temperatures. *Advanced Physical Research*, 2021, vol. 3, no. 3, pp. 147–152.
41. Aliyeva N.A., Aliyev Y.I., Abiyev A.S. Study of thermal properties of $Cu_4Se_{1.5}Te_{0.5}$ and $Cu_4Te_{1.5}Se_{0.5}$ compounds by differential thermal analysis. *Advanced Physical Research*, 2022, vol. 4, no. 2, pp. 94–99.
42. Normuradov M.T., Bekpulatov I.R., Imanova G.T., Igamov B.D. Structures for constructing devices from formed Mn_4Si_7 and CoSi films. *Advanced Physical Research*, 2022, vol. 4, no. 3, pp. 142–154.

32. Umirzakov B.E., Imanova G.T., Bekpulatov I.R., Turapov I.Kh. Obtaining of thin films of manganese silicides on a Si surface by the method of solid-phase deposition and investigation of their electronic structure // Modern Physics Letters B. 2023. V. 37. N 24. P. 2350078. https://doi.org/10.1142/S0217984923500781
33. Mansimov Z., Imanova G., Garibov A., Agayev T. Investigation of radiation-heterogeneous and catalytic processes in the surface of $(RaO)x(SiO_2)y + H_2O$ system // Journal of the Turkish Chemical Society Section A: Chemistry. 2023. V. 10. N 2. P. 487–492. https://doi.org/10.18596/jotcsa.1118855
34. Barkaoui S., Chakhari S., Kouass S., Dhaouadi H., Imanova G., Touati F. Influence of Ag-doping-cobalt oxide on the structure, optical properties, morphology and preferential oxidation activity of CO // Advanced Physical Research. 2022. V. 4. N 1. P. 22–32.
35. Canpolat G., Ziyadanoğullari R. Recovery of copper from complex copper oxide ore by flotation and leaching methods // Advanced Physical Research. 2023. V. 5. N 2. P. 103–116.
36. Teng F., Chen M., Li G., Teng Y., Xu T., Hang Y., Yao W., Santhanagopalan S., Meng D.D., Zhu Y. High combustion activity of CH_4 and catalluminescence properties of CO oxidation over porous Co_3O_4 nanorods // Applied Catalysis B: Environmental. 2011. V. 110. P. 133–140. https://doi.org/10.1016/j.apcatb.2011.08.035
37. Che H., Liu A., Fu Q., Jiang R. Facile synthesis of porous cobalt oxide microdiscs and their catalytic property in CO oxidation // Materials Letters. 2013. V. 93. P. 240–243. https://doi.org/10.1016/j.matlet.2012.11.108
38. Barkaoui S., Imanova G. Hydrothermal synthesis of Co3O4 urchin-like and their catalytic properties in CO oxidation // Juniper Online Journal Material Science. 2022. V. 7. N 1. P. 555704. https://doi.org/10.19080/jojms.2022.07.555704
39. Popov E.P., Aliyev O.A., Demir E., Neov D., Doroshkevich A.S., Mirzayev M.N., Horodek P., Thabethe T.T., Imanova G.T., Akhundzada H.V., Sidorin A.A., Mamedov F. Kinetics of thermo heterogeneous process under non-isothermal terms on the titanium carbide: a study on the different irradiation conditions // Advanced Physical Research. 2022. V. 4. N 2. P. 81–86.
40. Aliyev Y.I., Dashdemirov A.O., Novruzov R.F. Structural phase transitions in the compound $Ag_{1.55}Cu_{0.45}S$ at high temperatures // Advanced Physical Research. 2021. V. 3. N 3. P. 147–152.
41. Aliyeva N.A., Aliyev Y.I., Abiyev A.S. Study of thermal properties of $Cu_4Se_{1.5}Te_{0.5}$ and $Cu_4Te_{1.5}Se_{0.5}$ compounds by differential thermal analysis // Advanced Physical Research. 2022. V. 4. N 2. P. 94–99.
42. Normuradov M.T., Bekpulatov I.R., Imanova G.T., Igamov B.D. Structures for constructing devices from formed Mn_4Si_7 and CoSi films // Advanced Physical Research. 2022. V. 4. N 3. P. 142–154.

Author

Gunel Imanova — PhD (Physics), Associate Professor, Leading Researcher, Institute of Radiation Problems, Ministry of Science and Education Republic of Azerbaijan, Baku, AZ1143, Azerbaijan; Scientific Researcher, UNEC Research Center for Sustainable Development and Green Economy named after Nizami Ganjavi, Baku, AZ1001, Azerbaijan, SC 56272342000, https://orcid.org/0000-0003-3275-300X, gunel_imanova55@mail.ru

Автор

Иманова Гюнель — PhD (физические науки), доцент, ведущий научный сотрудник, Институт Радиационных Проблем, Министерство науки и образования Азербайджанской Республики, Баку, AZ1143, Азербайджан; научный исследователь, Исследовательский центр UNEC по устойчивому развитию и зеленой экономике имени Низами Гянджеви, Баку, AZ1001, Азербайджан, SC 56272342000, https://orcid.org/0000-0003-3275-300X, gunel_imanova55@mail.ru

Received 28.07.2023
Approved after reviewing 27.08.2023
Accepted 10.11.2023

Статья поступила в редакцию 28.07.2023
Одобрена после рецензирования 27.08.2023
Принята к печати 10.11.2023